SUPPLEMENTAL METHODS AND INFORMATION

Host Based Lipid Inflammation Drives Pathogenesis in *Francisella* Infection

Alison J. Scott[1], Julia Maria Post[2], Raissa Lerner[2], Shane R. Ellis[3], Joshua Lieberman[4], Kari Ann Shirey[5], Ron M.A. Heeren[3], Laura Bindila[2], Robert K. Ernst[1*]

[1] Department of Microbial Pathogenesis, School of Dentistry, University of Maryland, Baltimore, MD 21201, USA

[2] Laboratory for Eicosanoids and Endocannabinoids, Johannes Gutenberg University Mainz, DE

[3] M4I, The Maastricht MultiModal Molecular Imaging Institute, Maastricht University, 6229 ER, Maastricht, NL

[4] Department of Pathology, University of Washington Medical Center, Seattle, WA 98118, USA

[5] Department of Microbiology & Immunology, School of Medicine, University of Maryland, Baltimore, MD 21201, USA

Corresponding Author:
Robert K. Ernst
Department of Microbial Pathogenesis, School of Dentistry
University of Maryland, Baltimore
650 W. Baltimore St
Baltimore, MD 21201
rkernst@umaryland.edu
1 410 706 3622

SUPPLEMENTAL METHODS

METHODS

Bacterial strains and growth conditions for infections

Francisella novicida (*Fn*) strain U112 wildtype was grown in Tryptic Soy Broth (Sigma Aldrich, St. Louis, MO) containing 0.1% (w/v) L-cysteine (Sigma-Aldrich, St. Louis, MO) (TSBC). Agar plates were of the same composition with addition of 1.5% agar without antibiotic. Cultures were inoculated from frozen stocks onto TSBC agar plates and grown overnight at 37°C. A 5mL TSBC liquid culture was inoculated for expansion at 37°C, overnight. Three hours prior to infection a large volume subculture (1:37.5) was inoculated and grown for three hours. Bacteria were harvested by centrifugation and resuspended in sterile phosphate buffered saline (PBS) (Lonza, Walkersville, MD) for measurement of optical density. Infectious dose estimates were calculated for 300 CFU/dose (50uL), serial dilutions and final inoculum were suspended in sterile PBS. Final inoculum was enumeratred (colony forming units, CFU) in duplicate 10 µL drops on agar plates. All cultures for infection were grown at 37°C with orbital shaking at 225RPM. Infections with *Fn* ΔlpxD1 were performed according to the methods previously described by Li *et al*. (1) Briefly, inoculum was prepared as above with 5.5 x 10^6 organisms per dose (SQ) in PBS confirmed by CFU plating. Lipid A phenotype of *Fn* ΔlpxD1 inoculum was verified at *m/z* 1609 according to the published rapid lipid A extraction method. (2)

Mouse infections and tissue collection

Adult, female C57BL/6 mice were obtained from Jackson Laboratories. COX-2 knockout (*Ptgs2*$^{-/-}$) mice (3) were a generous gift from Dr. Stefanie Vogel (University of Maryland School of Medicine). Mice were housed in aBSL2 microisolator caging with negative pressure flow. Food

and water were provided *ad libitum*. Infectious material was delivered subcutaneously (SQ) using a tuberculin syringe and animals were monitored twice daily for signs of morbidity/mortality as well as recording of clinical progression scores. Mice were euthanized by carbon dioxide narcosis and secondary thoracotomy; tissues were excised post-mortem for MALDI-MSI. Tissues were collected every twelve hours through the lethal time point at seventy-two hours post infection. All studies were performed under humane guidelines according to the Institutional Care and Use Committee of the University of Maryland, Baltimore, under an approved protocol. The following criteria were used to assign clinical scores: 0-shiny coat, active, responsive to handling and tightly grasp cage top; 1-slight lethargy, but still shiny coat, readily release hold of cage top on handling; 2-decreased responsiveness to handling, mild to moderate piloerection, general lethargy; 3-decreased activity, ruffled or scruffy coat, marked loss of grooming activity, hunched posture, rapid shallow breathing; 4-inactive and unresponsive, weak or ataxic; 5-deceased.

Tissue preparation for MSI and histology

Tissues for two-dimensional (2D) MALDI-MSI were frozen at a controlled rate using a foil float in a liquid nitrogen pool. MALDI-MSI tissues were sectioned at 10 μm thickness (for 2D TOF experiments) and 13 μm thickness (for FTMS and 3D reconstruction experiments) on a Leica cryomicrotome (Buffalo Grove, IL). Thin sections were moved to slides with brushes and heat mounted in place at 37°C. Tissues for three-dimensional (3D) MALDI-MSI were formalin fixed (10% neutral buffered formalin) for eighteen hours and switched to PBS. Fixed tissues were snap frozen prior tocryosectioning. Fixed sections were cut to 13 μm thickness and heat mounted as above. Following MSI, sections were stripped of matrix in 70% ethanol and stained by

hematoxylin and eosin (H&E) as previously described. (4) Tissues for pathology were fixed for eighteen hours then embedded in paraffin. Thin formalin-fixed paraffin-embedded (FFPE) sections were cut and stained by the University of Maryland, Baltimore Medical School Histology Core. Digital scans of all H&E stained slides were captured on an Aperio Slide Scanner and visualized in ImageScope software (Aperio, Leica Microsystems, Buffalo Grove, IL).

Histology of infected spleens

A Resident Physician in Anatomic Pathology (Dr. Joshua Lieberman) analyzed fourteen blinded spleen scans from a SQ infection with *Fn* . Two spleens representing biological replicates at seven different time points (naïve, 12, 24, 36, 48, 60, 72) hours post infection (h.p.i.) were analyzed and reported prior to unblinding. Following routine formalin fixation and tissue processing, two 8 μm sections for each spleen were cut, stained by Hematoxylin & Eosin, and scanned to digital image files using Aperio Image Scope software. Digital slide images of spleen sections were evaluated for white pulp and red pulp architecture, as well as cell population and cytology; bacteria were noted when applicable. Presence of Gram-negative organisms in the *Fn* infected spleens was confirmed using the Brown and Brenn staining kit (American MasterTech, Lodi, CA).

2D MALDI-TOF-MSI

For MALDI-TOF-MSI, thin tissue sections mounted on ITO slides (above) were sprayed with matrix for imaging as follows: lipid A imaging – 12 mg/mL norharmane (NRM) in 2:1:0.5 (v:v:v) chloroform:methanol:water (**Fig. 1**); phospholipid imaging – 10 mg/mL NRM in 1:2:0.5

(v:v:v) chloroform:methanol:water (**Fig. 2**). (4,5) In both cases, approximately 10 mL total volume was applied in an ImagePrep (Bruker, Billerica, MA) nebulization device. Lipid A images were captured in negative ion mode on an UltraFlex MALDI-TOF/TOF(Bruker, Billerica, MA) with 75 μm rastering over a mass range of *m/z* 600-1700. Phospholipid images were captured in negative ion mode at 75 μm resolution over a mass range of *m/z* 600-1500. Calibration to 50 ppm was performed on a peptide calibrant spotted on the slide in NRM matrix. All time course tissues were mounted on the same ITO slide and captured in arbitrary order to avoid collection order bias and effects from matrix sublimation during capture. SAPI fragmentation analysis was performed on-tissue by MALDI-TOF/TOF (UltraFlex) in negative ion mode. Images were captured and analyzed using flexImaging (Bruker, Billerica, MA). Images were normalized to total ion current (TIC) and visual display range was optimized (using a frequency vs. intensity histogram) for each mass feature shown. Both *m/z* 1665 (lipid A) and *m/z* 885.6 (SAPI) images (**Figs. S14, S15; respectively**) are given as monocolor TIC normalized data (a), monocolor TIC normalized data showing region of interest (ROI) capture area outlines (b), monocolor unnormalized data (c), and as multicolor scale TIC normalized data (d) for maximum transparency of image preparation, analysis, and interpretation. Images (histology and MSI) were exported as .tiff files and cropped for presentation in GIMP (GNU Image Manipulation Program v2.8.10, www.gimp.org). Global enhancement of SAPI and lipid A images were applied (10% brightness optimization) uniformly in **Figs. 1** and **2** in post-analysis to ensure fidelity of print to the electronically displayed data, **Figs. S14, S15** are the underlying images, unmodified for reference.

3D MALDI-TOF-MSI

For 3D MALDI-TOF MSI reconstructions fixed tissues were sectioned and heat-mounted to ITO as above. Tissues were prepared for imaging using a SunChrom Sprayer Device (SunCollect, Napa, CA) using the same matrix solutions as above and deposition according to previously described methods by Scott *et al*. (4) Imaging was performed in negative ion mode at 20 μm rastering, 200 shots per raster position, on a Bruker RapiFlex (6) MALDI-TOF/TOF (Billerica, MA). Instrument was externally calibrated prior to each MSI acquisition using to red phosphorus clusters. Final 3D reconstruction was performed in SCiLS software (7) (SCiLS Lab v 2016a, Bremmen, DE), composed of 16 serial sections of spleen cut from the central third of the tissue from infection at 48 h.p.i., an area roughly 0.75 cm x 0.75 cm. All images were imported into SCiLS and normalized to TIC for use in 3D image reconstruction. Video rendering of single ion channel volume views were performed in the same manner.

2D MALDI-FTICR-MSI

MALDI-TOF 2D MSI results were confirmed using MALDI-FTICR MSI using the same tissue preparation steps as above for MALDI-TOF, except that tissues were cut to 13 μm thickness. Data was captured according to previously described conditions by Scott *et al*. (4) Briefly, a Bruker solariX 12T MALDI-FTICR (Billerica, MA) was calibrated to 1ppm using sodium trifluoroacetate clusters in negative ion mode, data was collected at 75 μm rastering with 100 shots per raster. Spectral data were processed for images in flexImaging (Bruker Daltonics, Billerica, MA), normalized to TIC.

Quantitation of eicosanoids and phospholipids using LCMS MRM methods

Extraction and quantification of PLs and eicosanoids was carried out as previously described (8) from approximately 5mg portions each of spleen. Care was taken to ensure the extracted spleen portion was taken from the center of the tissues by first bisecting the frozen spleens and snapping a frozen portion away with a clean razor blade. All spleen portions were weighed and total protein quantitated (BCA assay) according to manufacturer's instructions (ThermoPierce) for normalization purposes prior to extraction. Lipid Maps (9) quantitative standards were spiked into extraction from a common master mix containing each lipid class to be analyzed.

Quantitative RT-PCR

Total RNA was extracted from spleens according to previously described methods. Results are presented at log2 fold changes in transcript abundance over naïve (mouse transcripts). Data was analyzed according to previously established methods. Primer pairs for the *Il1b*, *Tnfa*, *Pla2*, and *Ptgs2,* and *Hprt* gene products were established previously. (10) 16S (F-GTTACCCAAAGAATAAGCACCG, R-AAATTCCCCATTCCTCTACCG and dnaK (F-GGACAAACTCGTATGCCTCTAG, R-CACCTCCCATAGTCTCAATACC) primers for the corresponding *Fn* gene products were designed in using RealTime PCR Design Tool (IDT, Coralville, IA). Bacterial expression data were analyzed using the copy count method. Significance was evaluated using the Student's t-test, *p* values are given in legends.

Confirmation of lipid A structure in spleen

Lipid A structure from total lipid extracts (performed according to Scott *et al*) (4) of infected mouse spleens was confirmed via tandem mass spectrometry. Briefly, the lipid extract was

mixed with 1:1 with norharman matrix solution (v:v) and 1 μL deposited onto an ITO slide. MS/MS and MS^3 fragmentation data were acquired on an Orbitrap Elite (Thermo Fisher Scientific GmbH, Bremen, Germany) mass spectrometer coupled to an intermediate pressure (~7.5 torr) MALDI ion source (Spectroglyph LLC, Kennewick, WA, USA) MS/MS and MS^3 fragmentation data were collected using collision-induced dissociation (40, normalized energy, 1.5 Da window) with ion trap detection. Standard MS2 and MS3 fragmentation patterns for *Fn* lipid A established by Shaffer *et al* (11) were readily identified. Further, we evaluated an alternative fragmentation pattern (**Fig. S4**, redrawn from Shaffer *et al*) to confidently assign the major lipid A structure in **Fig. 1b**. MALDI and trapping conditions were as follows: 1 μL of total lipid extract was spotted on a MALDI target with 1 μL norharmane in 2:1 choloroform:methanol (v:v).

SUPPLEMENTARY INFORMATION

Table S1: Lipid A fragmentation confirming host-adapted structure.

1665.2➔ MS2 Fragments (*m/z*)	**1665.2➔1424.9**[#] MS3 Fragments (*m/z*)
1504.2	1382.9
1424.9	1365.1
1408.9	1263.8
1364.8	1246.3
1248.0	1204.0
1203.8	1184.8
1124.7[*]	1168.8
1108.6	1124.9
947.7[*]	1108.8
921.6	1007.6
868.4[*]	963.8
707.3[*]	946.5
665.3	868.3
	707.4
	665.3

*Identifying fragments ions of 1665.2 per Shaffer *et al*.

#Minor fragment ion of 1665.2 produced alternative identifying fragmentation pattern.

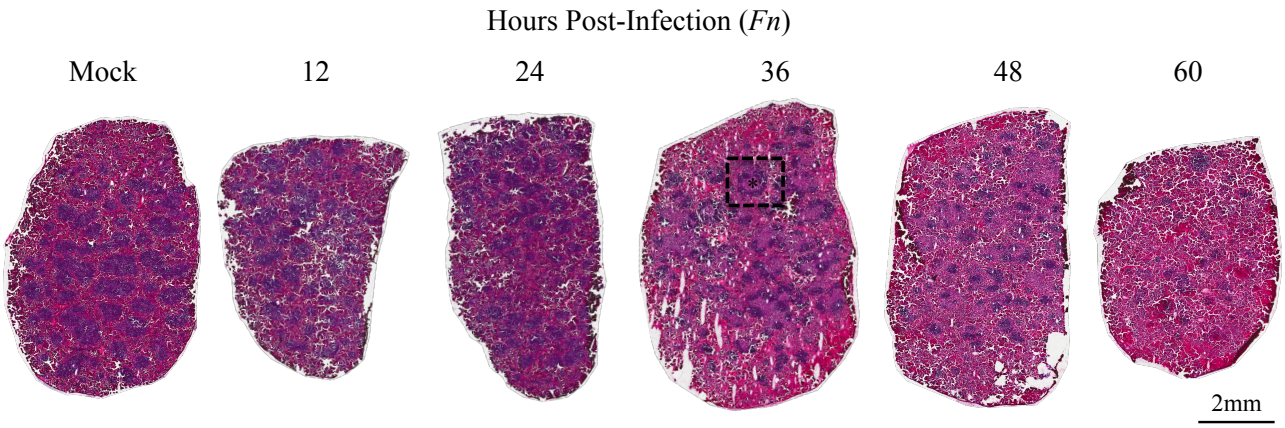

Figure S1: Tissue references for spleen MSI data. Tissue sections analyzed in **Fig 1a** stained by H&E for reference, black outlined box region references the location of an annotated white pulp nodule in serial sections analyzed in **Fig 2a**.

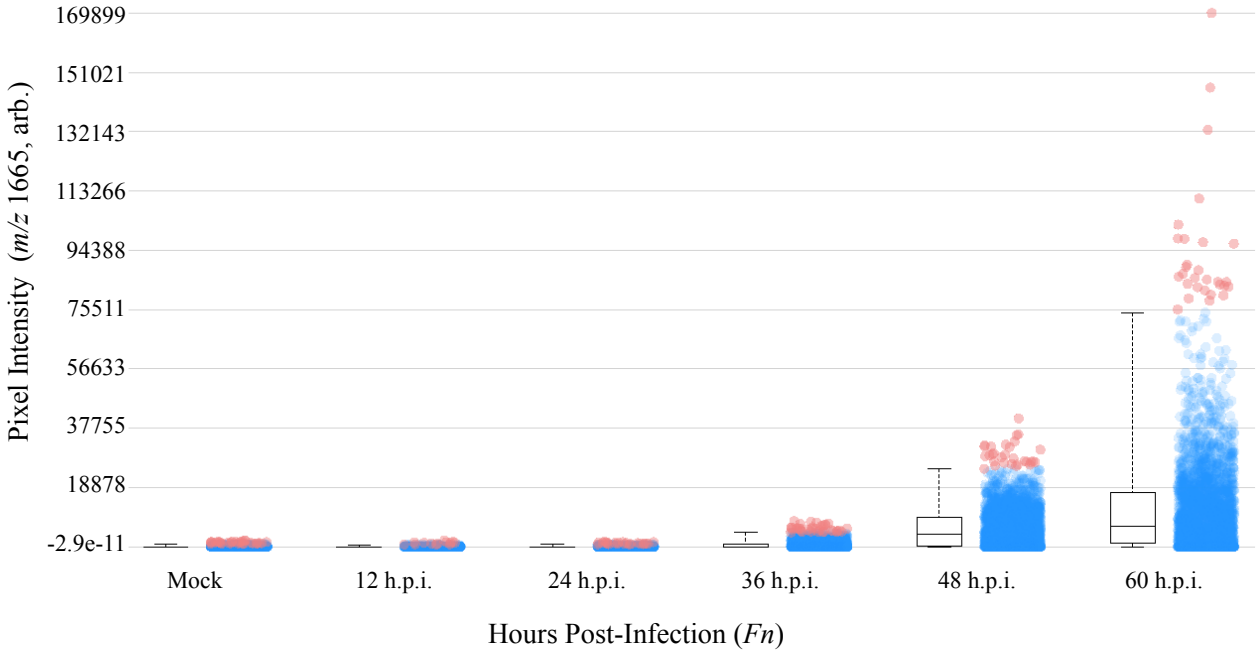

Figure S2: Pixel intensities of *Fn* lipid A across infection timecourse. Pixel intensity (arbitrary units, normalized, TIC) plotted for each timecourse condition from MALDI-FTICR validation studies of MALDI-TOF imaging data in **Fig. 1a**. Box and whisker plots given to the left representing a summation of the individual pixel intensities plotted on the right.

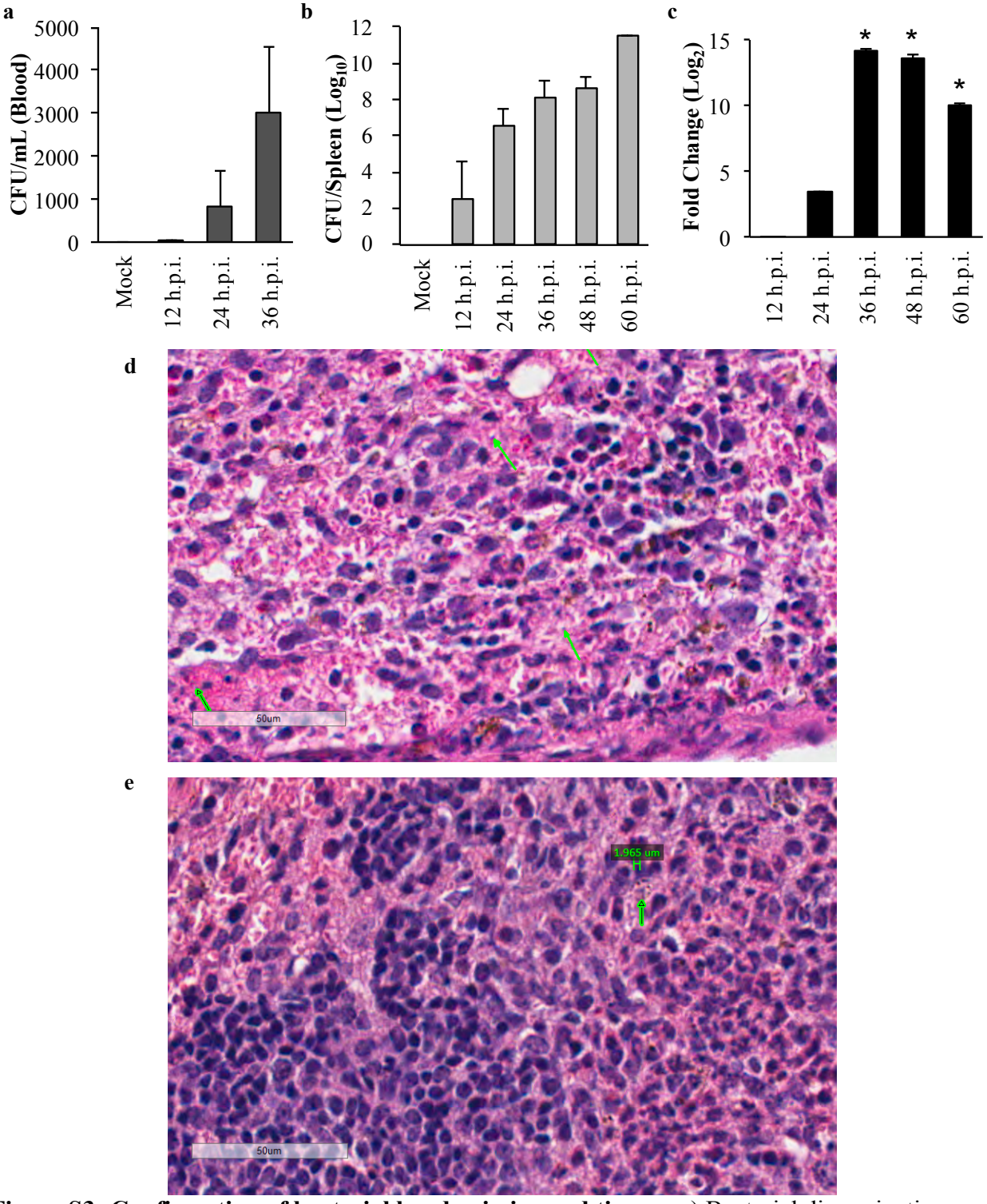

Figure S3: Confirmation of bacterial burden in imaged tissues. a) Bacterial dissemination (*Fn*), cardiac blood, postmortem**,** colony forming units (CFU) enumerated on TSBC agar plates from triplicate infections. b) Bacterial burden in spleens from a parallel experiment (363 CFU/dose, SQ). c) Confirmation of bacterial transcript in second half of bisected spleens from MSI panel, *Fn dnaK* transcript normalized to murine *Hprt*. n=3. a,b. Error bars = SD. d)

Representative identification of bacteria (green arrows) within infected spleens at 36 h.p.i., FFPE, H&E, 40x magnification, subcapsular red pulp. e) Measurement of *Fn* length in green at arrow tip, 1.965μm, intracellular, tissue same as c.

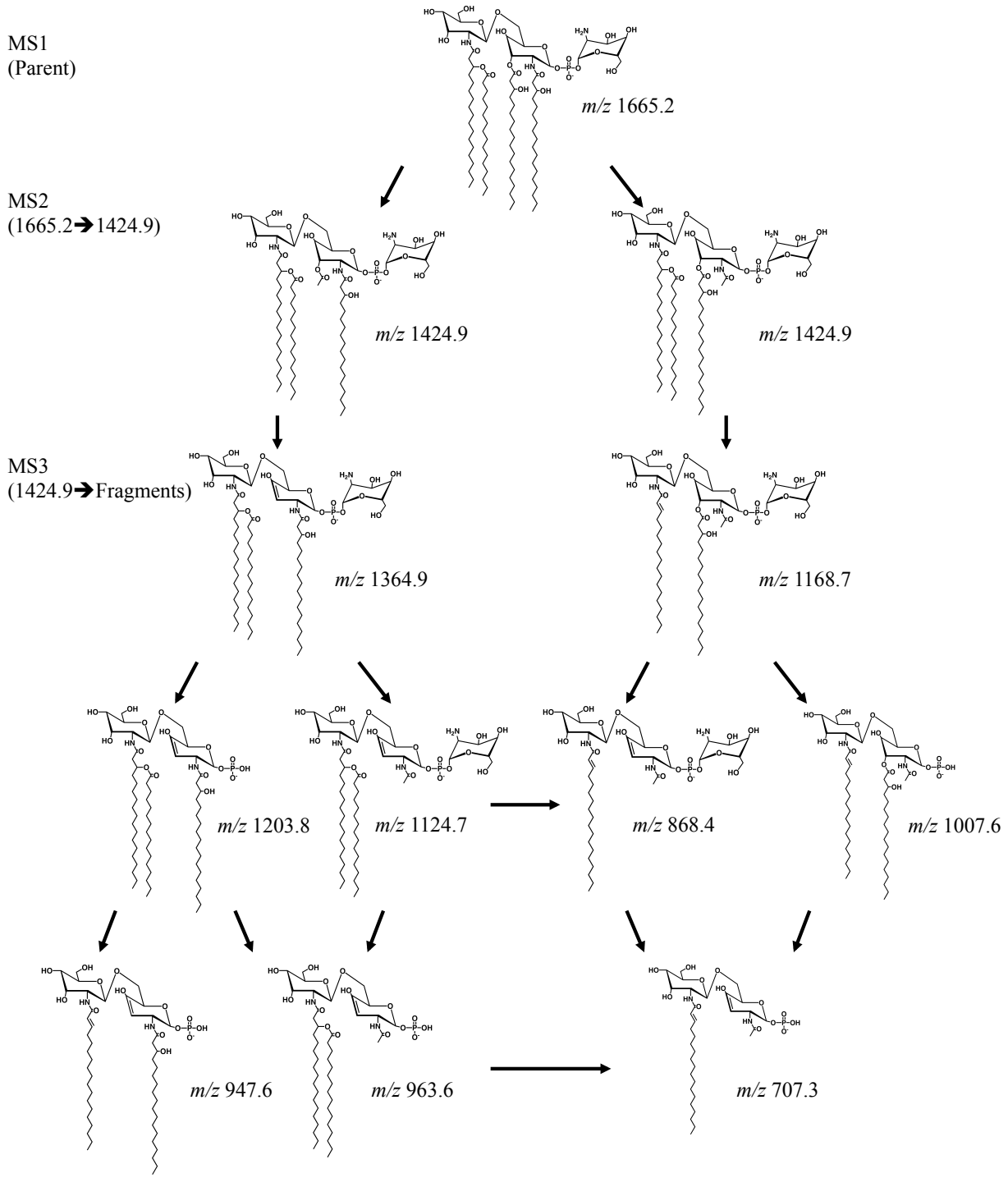

Figure S4: Alternative fragmentation pattern observed in *ex vivo* lipid A extracts confirming assigned structure. Redrawn with permission from Springer (License 4064251241606) from Shaffer *et al*[10], fragments from **Table S1**.

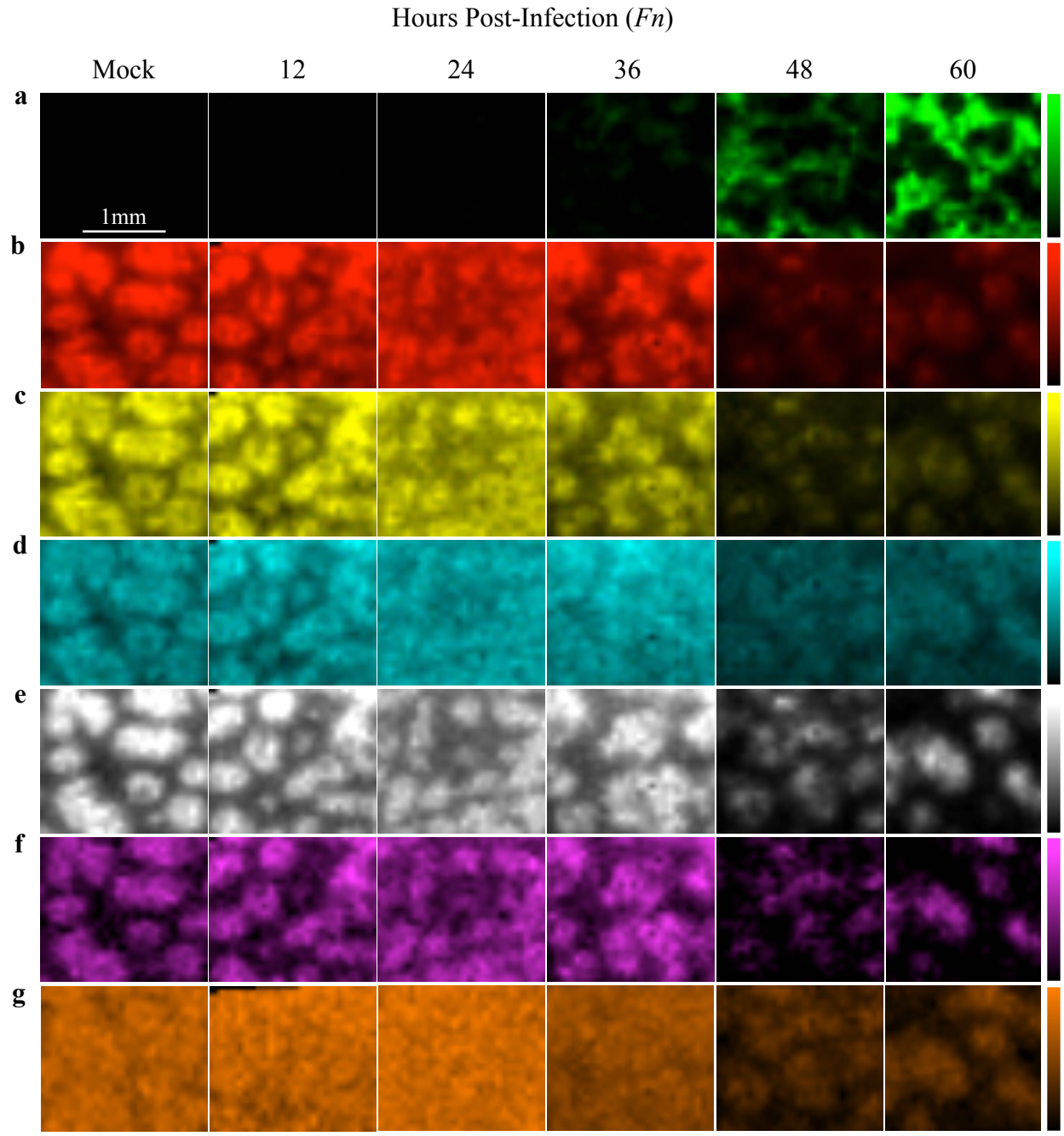

Figure S5: MALDI-FTICR high mass accuracy confirmation of MALDI-TOF MSI data; differential distribution of lipid A and six phospholipids following infection with *Fn*. Serial sections of tissues in **Figs. 1, 2**. a) Lipid A, green, *m/z* 1665.2, scale 0-50 (arbitrary intensity). b) SAPI, red, *m/z* 885.6, scale 0-1000. c) PI 36:4, yellow, *m/z* 857.5, scale 0-90. d) PI 34:1, cyan, *m/z* 835.5, scale 0-65. e) PE 38:4, white, *m/z* 766.5, scale 0-130. f) unassigned identity, magenta, *m/z* 763.5, scale 0-16, noted for unique white pulp nodule distribution. g) PA 38:4, orange, *m/z* 723.5, scale 0-32. a-b) identity confirmed by MS^n fragmentation. b-e, g) pattern and identity confirmed by LCMS.

226

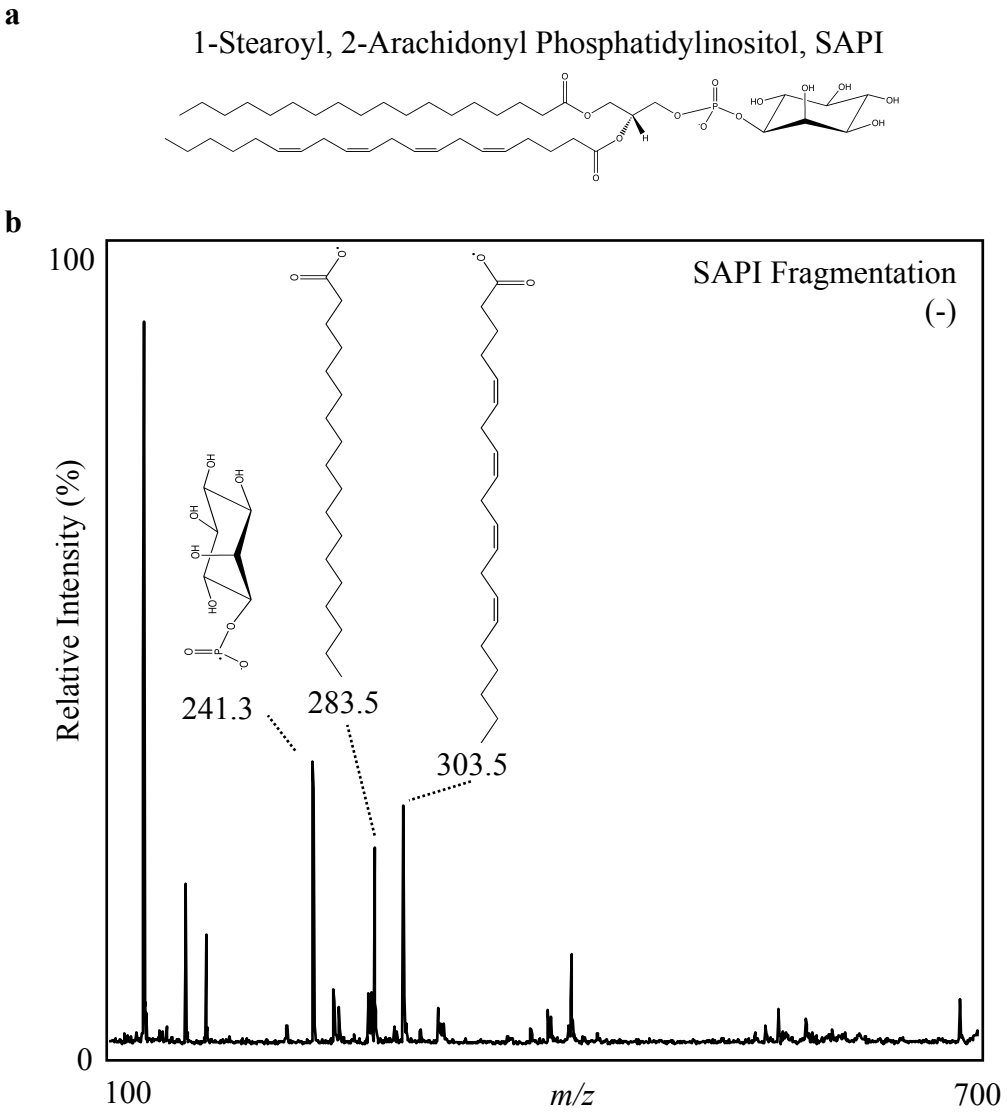

227
228

229 **Figure S6: Confirmation of SAPI Identity by tandem MS.** a) Predominant structure of *m/z*
230 885.7, SAPI. b) Fragment ion spectrum of parent peak *m/z* 885.7. Three characteristic fragments
231 for SAPI detected at *m/z* 241.3 (phosphoinositol headgroup), 283.5 (stearoyl fatty acid), and
232 303.5 (arachidonyl fatty acid). Negative mode MALDI-MS/MS.
233

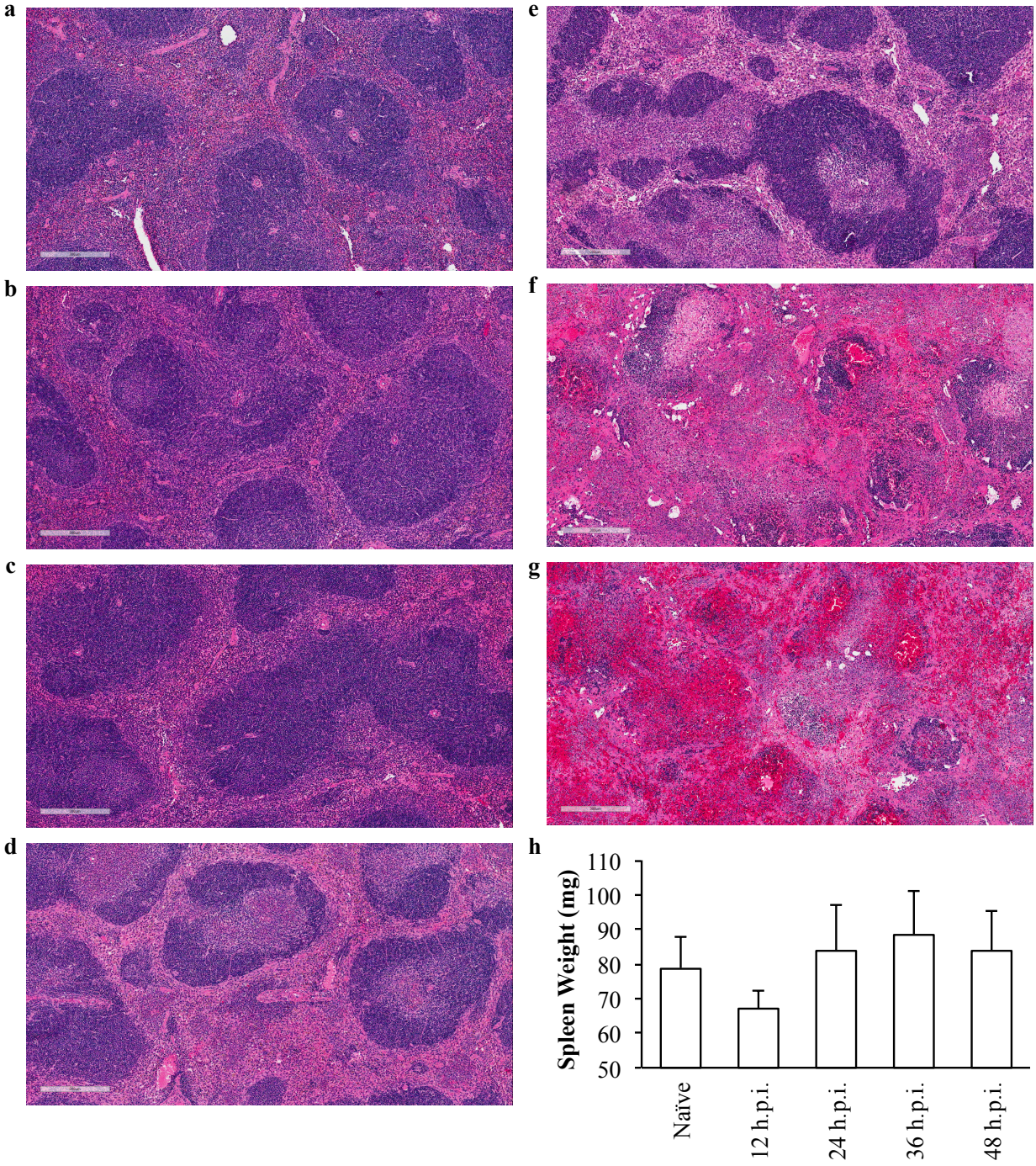

Figure S7: Histological evaluation of progressive tissue destruction in *Fn*-infected spleens. a-g) H&E stained FFPE spleen tissue excised from a lethal *Fn* timecourse infection. a) mock infected, b) 12 h.p.i., c) 24 h.p.i., d) 36 h.p.i., e) 48 h.p.i., f) 60 h.p.i., g) 72 h.p.i., representative of two replicate spleens at each timepoint. Scale bar: 300 μm. h) Total spleen weights over timecourse, n=10.

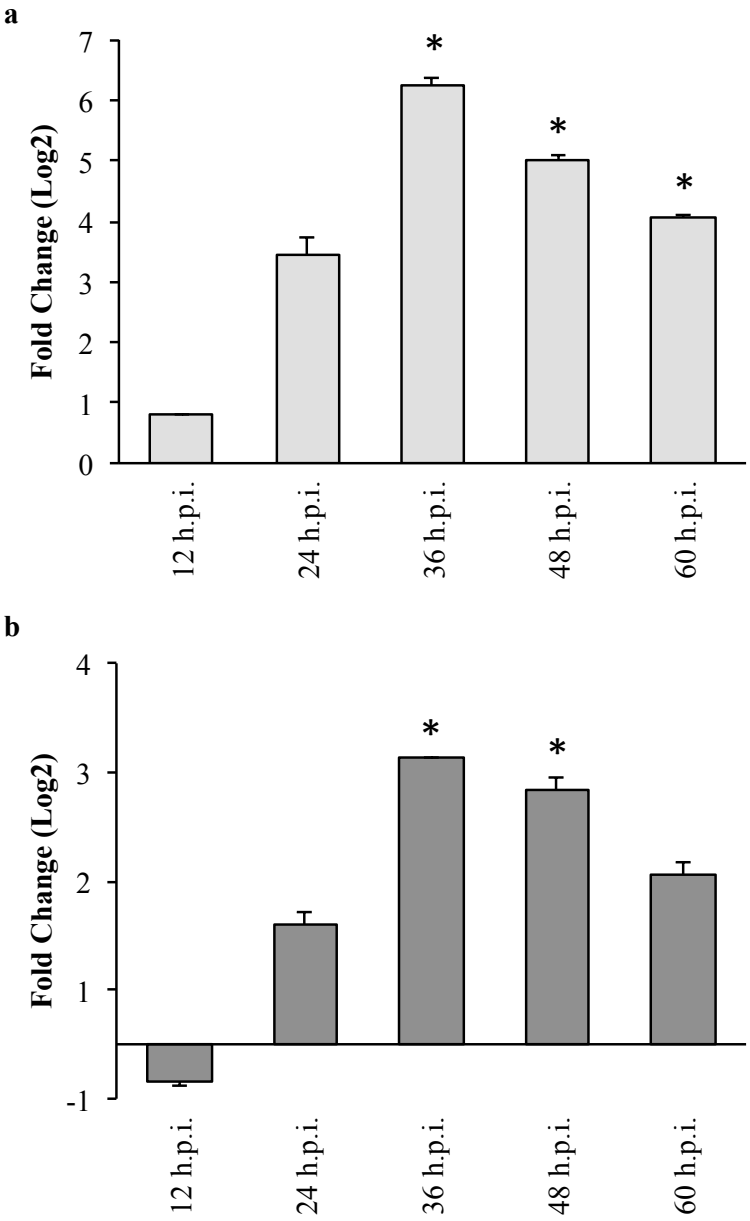

Figure S8: Confirmation of early phase inflammatory markers following *Fn* infection in mouse spleen. a-b) qRT-PCR of IL-1β and TNF-α, respectively, confirming activation of an innate immune reaction. Note, onset of fulminant infection coincides with peak production of IL-1β . Error bars = SD. n=3 per timepoint, * $p<0.005$ using student's T-test of ΔCT values.

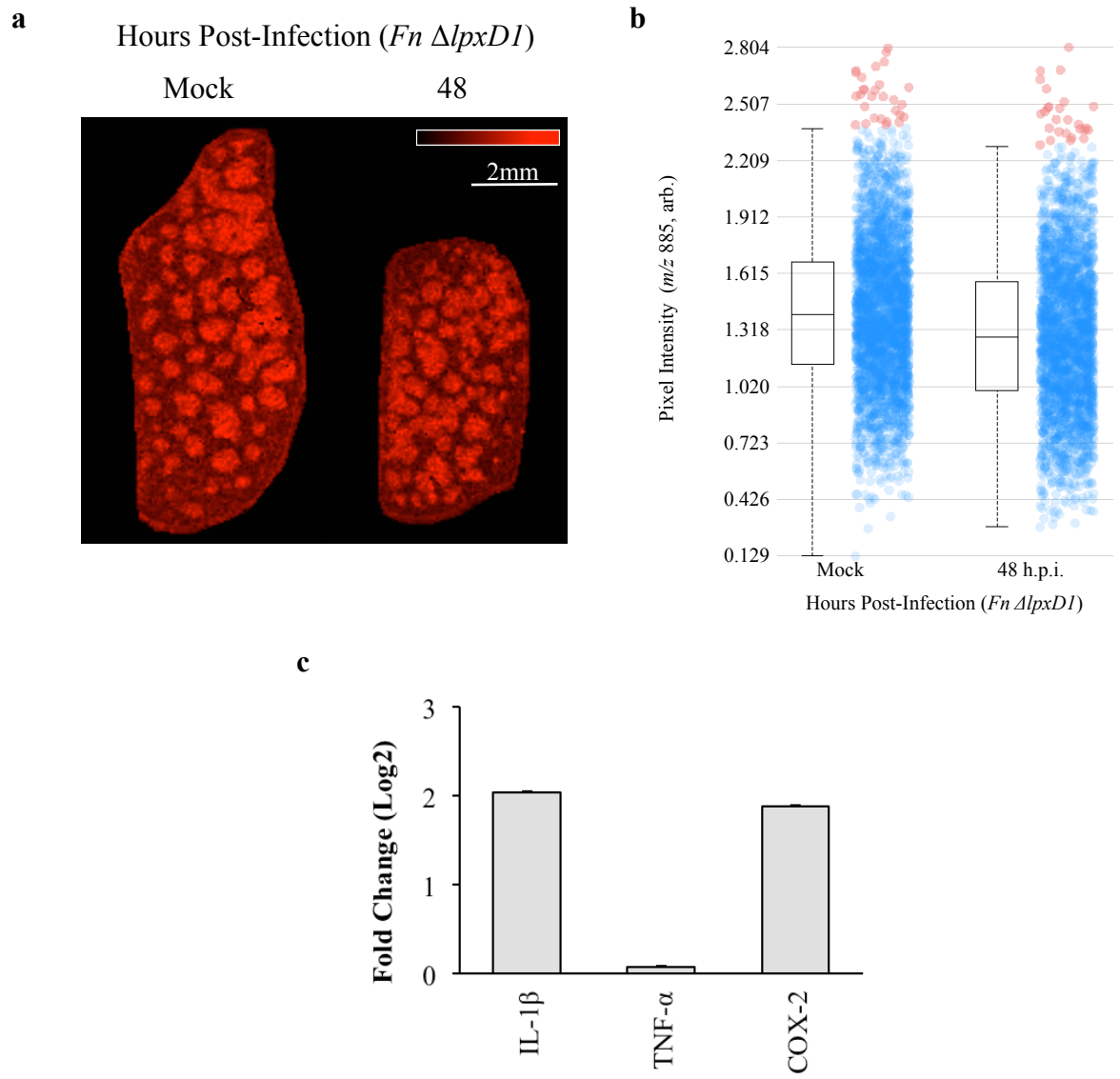

Figure S9: SAPI is not depleted in spleens infected with an avirulent mutant of *Francisella*. a) Negative ion mode image of *m/z* 885(SAPI), as in **Fig. 2a**, is shown in naïve and infected (*Fn* Δ*lpxD*1, 10^6 CFU, SQ) mouse spleens (13µm thickness), 75µm rastering, normalized to TIC, data representative of 3 independent biological replicates. b) Pixel intensity plot describing data in a). Box and whisker plots given to the left representing a summation of the individual pixel intensities plotted on the right. c) qRT-PCR quantitation of innate markers IL-1β and TNF-α alongside COX-2 48 h.p.i. (*Fn* Δ*lpxD*1) versus mock infected spleens, n=4. Normalized to mouse *Hprt*.

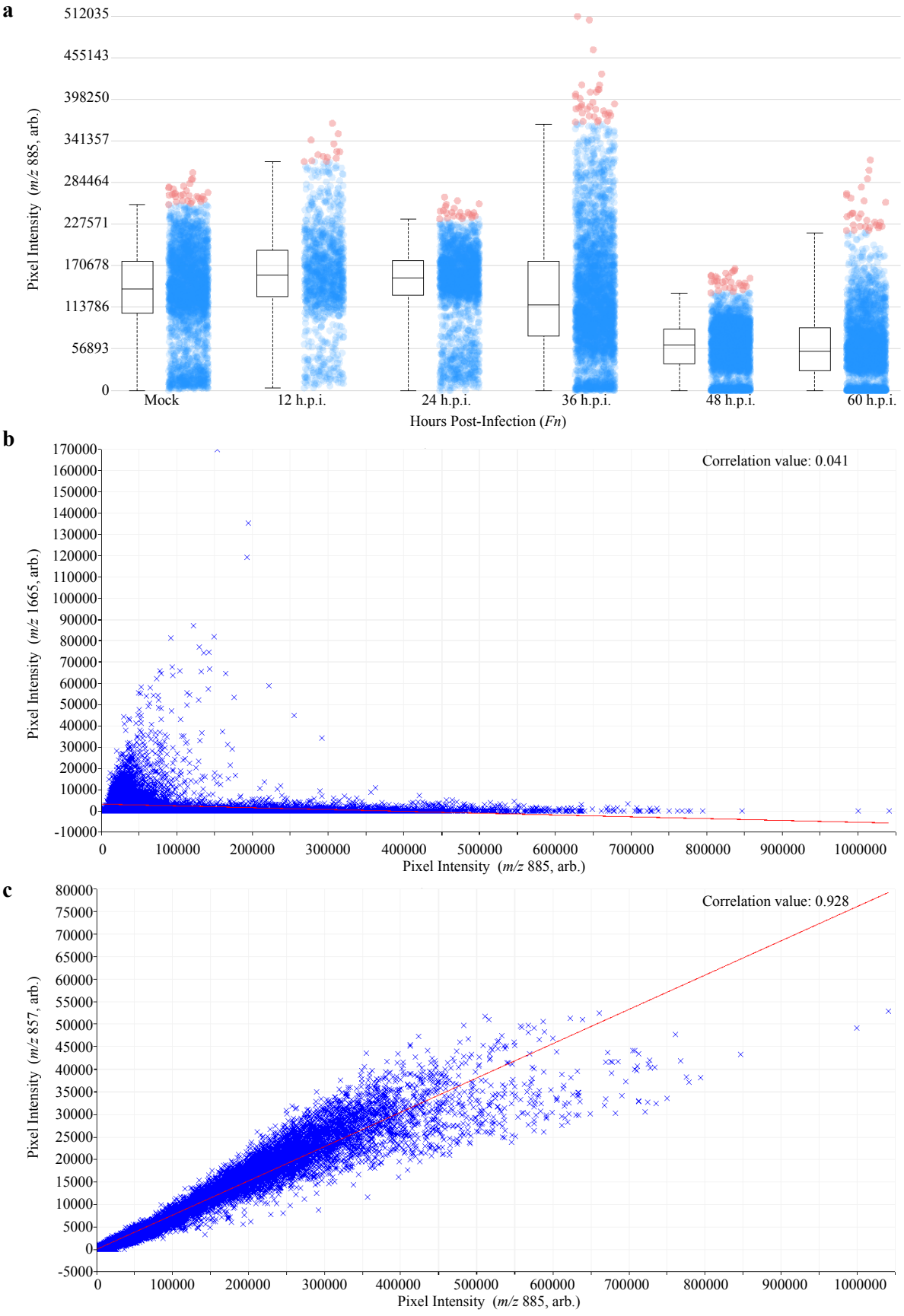
a
512035
455143
398250
341357
284464
227571
170678
113786
56893
0
Pixel Intensity (m/z 885, arb.)
Mock
12 h.p.i.
24 h.p.i.
36 h.p.i.
48 h.p.i.
60 h.p.i.
Hours Post-Infection (Fn)
b
Correlation value: 0.041
Pixel Intensity (m/z 1665, arb.)
Pixel Intensity (m/z 885, arb.)
c
Correlation value: 0.928
Pixel Intensity (m/z 857, arb.)
Pixel Intensity (m/z 885, arb.)

263

Figure S10: Pixel intensities of SAPI across infection timecourse and correlation plots of lipid A:SAPI and SAPI:PI 36:4. a) Pixel intensity (arbitrary units, normalized, TIC) plotted for each timecourse condition from MALDI-FTICR validation studies of MALDI-TOF imaging data in Fig. 2a. Box and whisker plots given to the left representing a summation of the individual pixel intensities plotted on the right. b) Pixel intensity correlation plot of SAPI versus lipid A for all pixels across entire timecourse, lipid A and SAPI have a correlation value of 0.041, no relationship. c) Pixel intensity correlation plot of two AA-bearing PI lipids: SAPI and PI 36:4 for all pixels across entire timecourse, SAPI and PI 36:4 have a correlation value of 0.982.

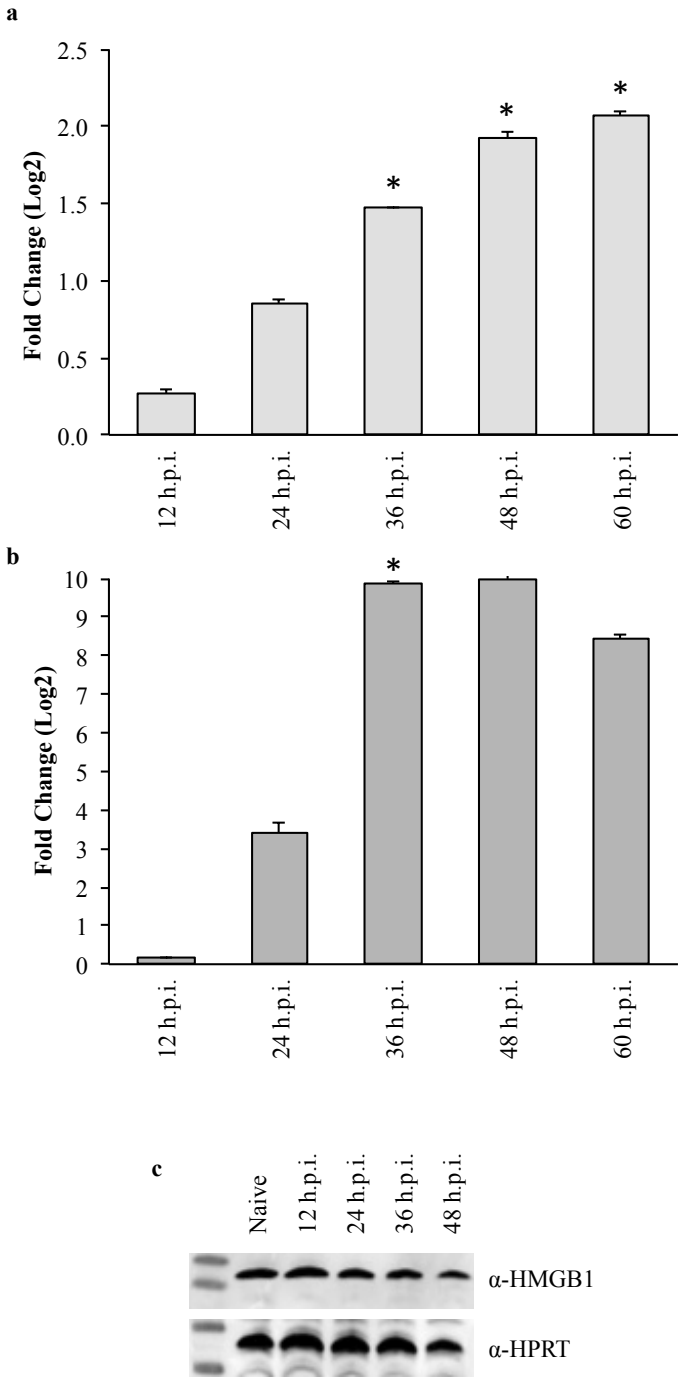

Figure S11: Transcriptional upregulation of genes involved in lipid mediated inflammation during *Fn* infection. a) qRT-PCR of *cPla2* gene (mouse *Hprt* control) across timecourse. b) qRT-PCR of *Ptgs2* gene (encoding COX-2; mouse *Hprt* control). Fold change expression and standard deviation. (n=3 per timepoint, * $p<0.005$ using student's T-test of ΔCT values. c) Western blot detection of splenic HMGB1, loading control HPRT. Total protein isolated from spleens across the twelve-hour timecourse, representative of results from two animals per group.

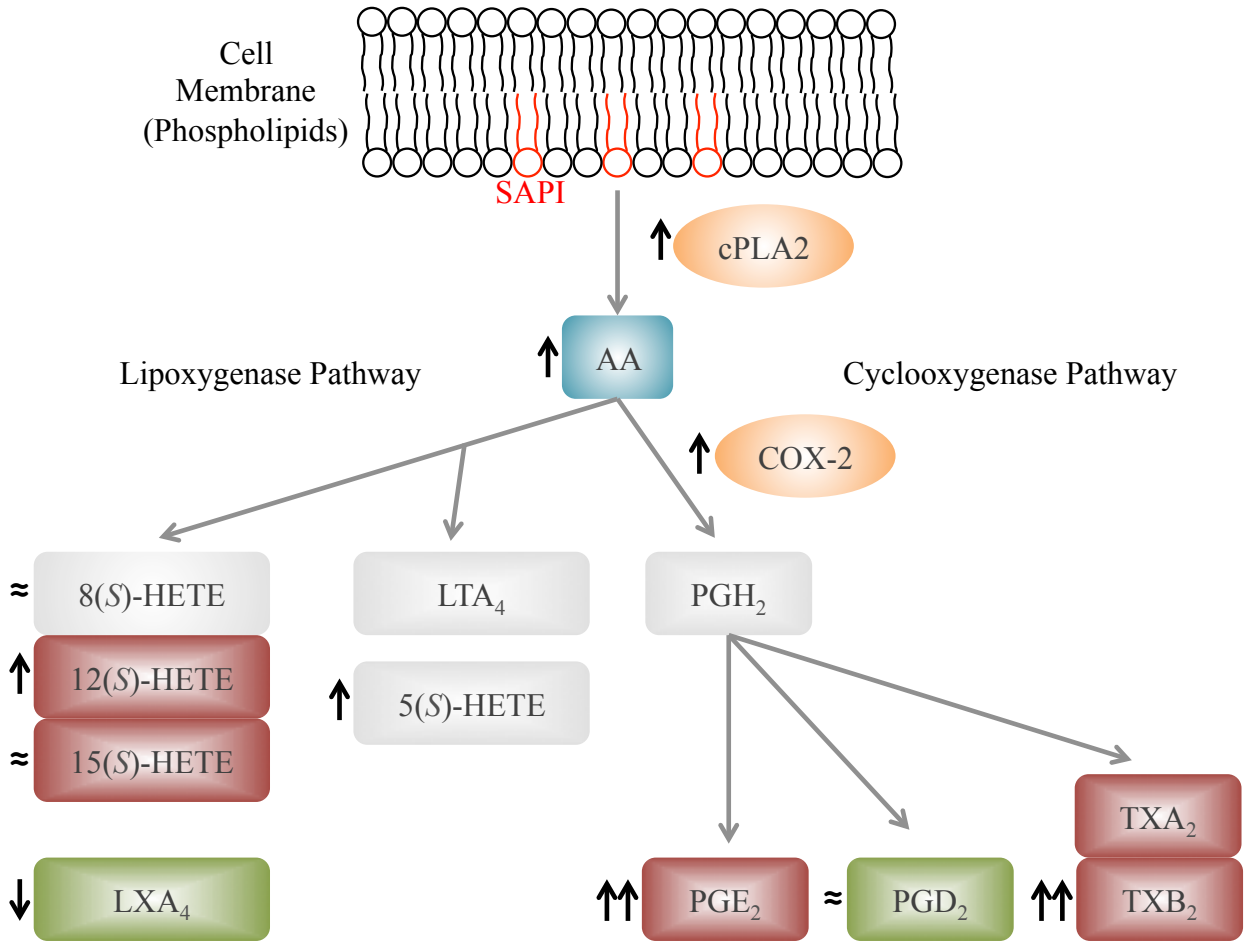

Figure S12: Regulatory schema of lipoxygenase (LOX) and cyclooxygenase (COX) pathways at 48 h.p.i. (*Fn*). Both cPLA2 and COX-2 (orange) are induced at 48 h.p.i. (data from **Fig. S11a-b**). AA is released from the membrane – from phospholipids such as SAPI and other AA-bearing lipids (data from Figs. **2a-b, 3a**). Metabolic products of COX and LOX are given at up- or down-regulated (arrow direction), as interpreted from LCMS data (PGE_2 and PGD_2 shown in **Fig. 3b-c**, remainder not shown). Single arrow = <5-fold change versus mock infected spleens; double arrows = >20-fold change versus mock-infected spleens. n=10. AA-derived products: red: upregulated; green, downregulated or no change; grey not tested.

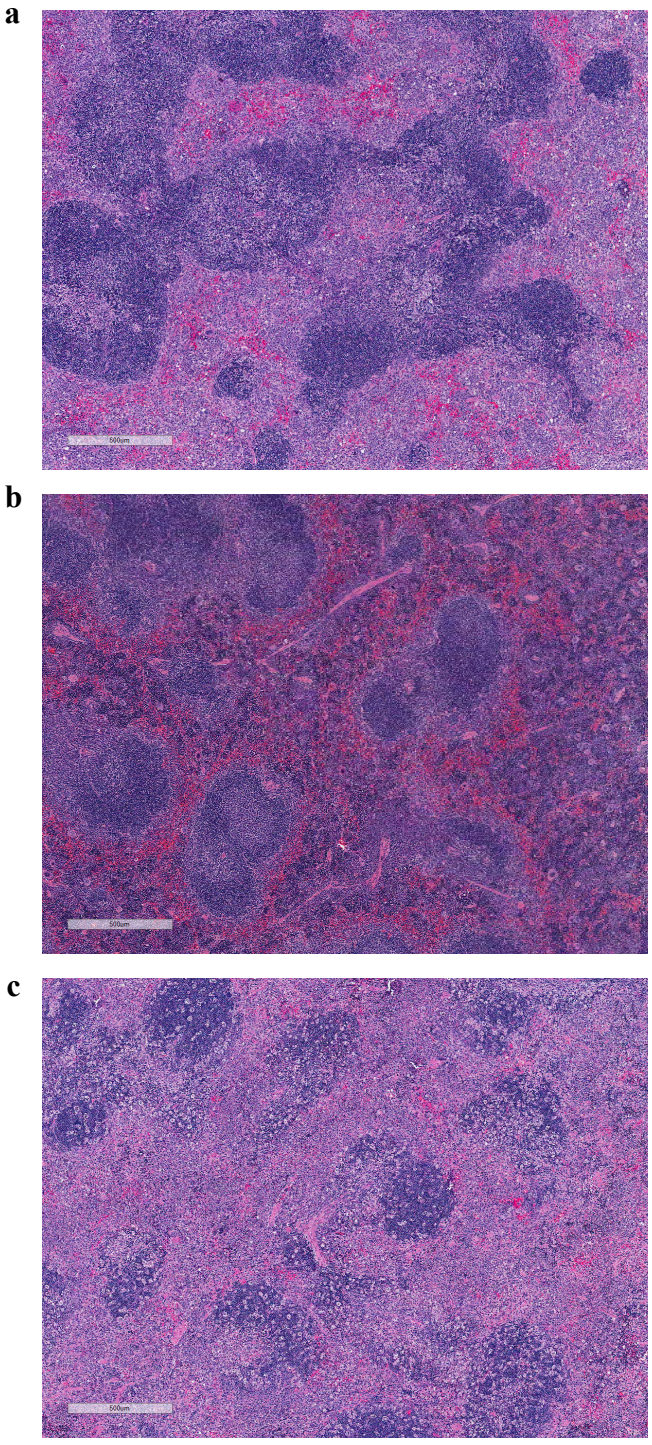

Figure S13: *Fn*-induced tissue pathology in COX-2 KO mice is less severe than in wildtype mice at the lethal timepoint (72 h.p.i.) for wildtype mice. a-c) Triplicate spleens from COX-2 KO mice infected with *Fn,* 72 h.p.i., H&E of FFPE tissue. Scale bar: 500 µm.

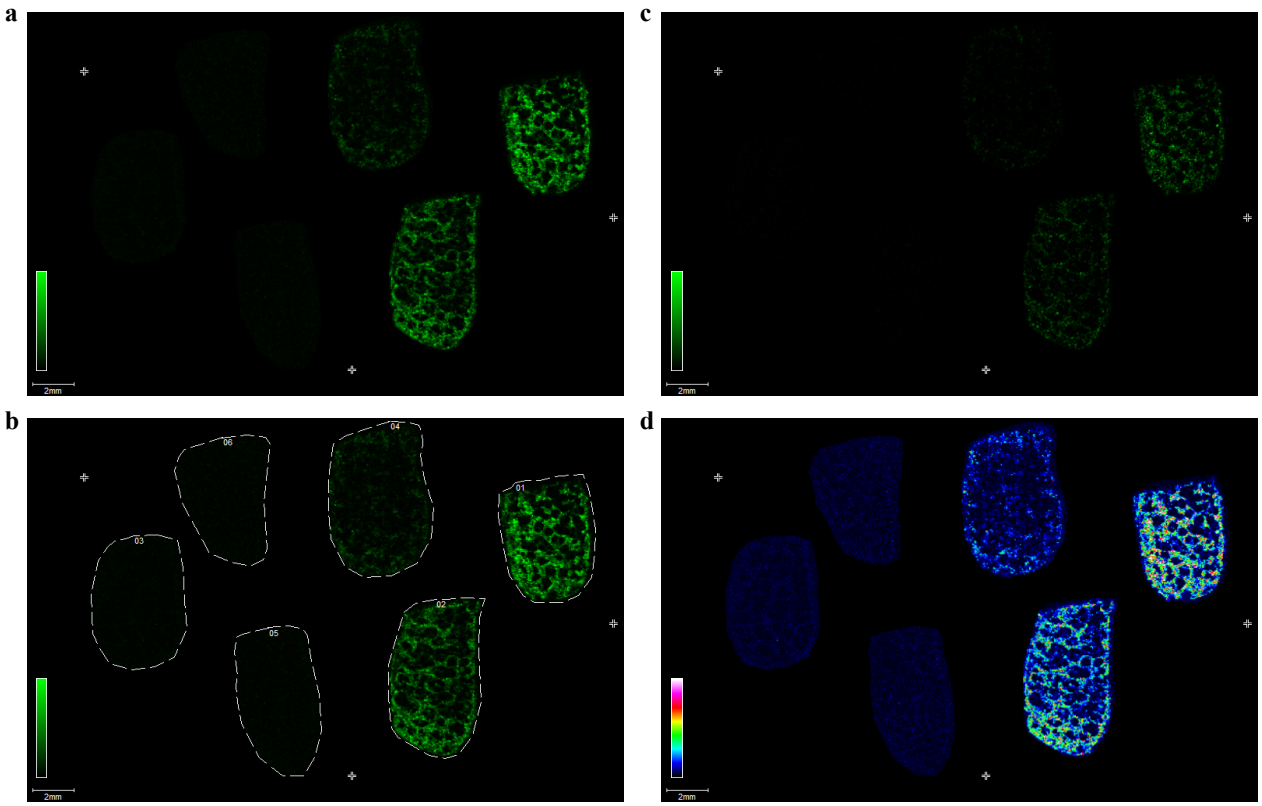

Figure S14: Data preparation for Figure 1a, MALDI-TOF. a) Uncropped image used for **Fig.1a**, normalized to TIC, unmodified for printing. For printing purposes the images in **Fig. 1a** had 10% contrast applied universally to match the contrast observed on-screen. b) Data from a) with collection regions outlined in white. c) Raw data, unnormalized. d) Data from a) shown on a multicolor scale.

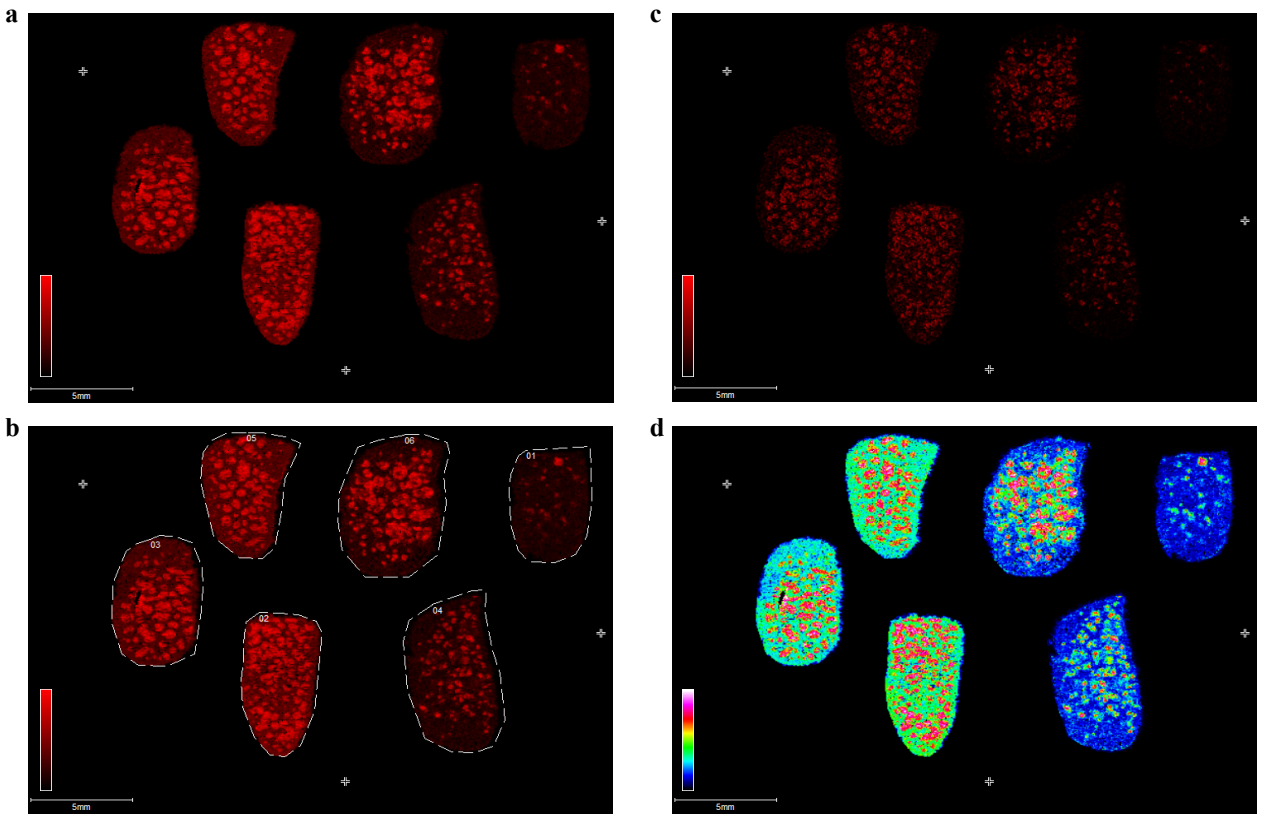

Figure S15: Data preparation for Figure 2a, MALDI-TOF. a) Uncropped image used for **Fig.2a**, normalized to TIC, unmodified for printing. For printing purposes the images in **Fig. 2a** had 10% contrast applied universally to match the contrast observed on-screen. b) Data from a) with collection regions outlined in white. c) Raw data, unnormalized. d) Data from a) shown on a multicolor scale.

REFERENCES

1. Li, Y. *et al.* LPS remodeling is an evolved survival strategy for bacteria. *Proc. Natl. Acad. Sci. U.S.A.* **109,** 8716–8721 (2012).
2. Li, Y., Wang, X. & Ernst, R. K. A rapid one-step method for the characterization of membrane lipid remodeling in Francisella using matrix-assisted laser desorption ionization time-of-flight tandem mass spectrometry. *Rapid Commun. Mass Spectrom.* **25,** 2641–2648 (2011).
3. Morham, S. G. *et al.* Prostaglandin synthase 2 gene disruption causes severe renal pathology in the mouse. *Cell* **83,** 473–482 (1995).
4. Scott, A. J., Flinders, B. & Cappell, J. Norharmane Matrix Enhances Detection of Endotoxin by MALDI-MS for Simultaneous Profiling of Pathogen, Host, and Vector Systems. *Pathogens and Disease* (2016).
5. Scott, A. J. *et al.* Mass spectrometry imaging enriches biomarker discovery approaches with candidate mapping. *Health Phys* **106,** 120–128 (2014).
6. Ogrinc Potočnik, N., Porta, T., Becker, M., Heeren, R. M. A. & Ellis, S. R. Use of advantageous, volatile matrices enabled by next-generation high-speed matrix-assisted laser desorption/ionization time-of-flight imaging employing a scanning laser beam. *Rapid Commun. Mass Spectrom.* **29,** 2195–2203 (2015).
7. Trede, D. *et al.* Exploring Three-Dimensional Matrix-Assisted Laser Desorption/Ionization Imaging Mass Spectrometry Data: Three-Dimensional Spatial Segmentation of Mouse Kidney. *Anal. Chem.* **84,** 6079–6087 (2012).
8. Lerner, R., Post, J., Loch, S., Lutz, B., Bindila, L. Targeting brain and peripheral plasticity of the lipidome in acute kainic acid-induced epileptic seizures in mice via quantitative mass spectrometry. *Biochim. Biophys. Acta.* **1862,** 255-267 (2017).
9. Fahy, E., Sud, M., Cotter, D. & Subramaniam, S. LIPID MAPS online tools for lipid research. *Nucleic Acids Research* **35,** W606–W612 (2007).
10. Cole, L. E. *et al.* Macrophage proinflammatory response to Francisella tularensis live vaccine strain requires coordination of multiple signaling pathways. *Journal of Immunology* **180,** 6885–6891 (2008).
11. Shaffer, S. A., Harvey, M. D., Goodlett, D. R. & Ernst, R. K. Structural heterogeneity and environmentally regulated remodeling of Francisella tularensis subspecies novicida lipid A characterized by tandem mass spectrometry. *J. Am. Soc. Mass Spectrom.* **18,** 1080–1092 (2007).